https://doi.org/10.61092/iaea.a8ym-9xyh

International Atomic Energy Agency

INDC(NDS)-0757
Distr. G+IN+J

INDC International Nuclear Data Committee

On the Benchmarking of INDEN Improved Iron Evaluations

A. Trkov
IAEA, Vienna, Austria

and

R. Capote
IAEA, Vienna, Austria

May 2018

IAEA Nuclear Data Section
Vienna International Centre, P.O. Box 100, 1400 Vienna, Austria

Selected INDC documents may be downloaded in electronic form
from *http://nds.iaea.org/publications*
or sent as an e-mail attachment.
Requests for hardcopy or e-mail transmittal should be directed to
NDS.Contact-Point@iaea.org
or to:
Nuclear Data Section
International Atomic Energy Agency
Vienna International Centre
PO Box 100
1400 Vienna
Austria

Printed by the IAEA in Austria

May 2018

INDC(NDS)-0757
Distr. G+IN+J

On the Benchmarking of INDEN Improved Iron Evaluations

A. Trkov
IAEA, Vienna, Austria

and

R. Capote
IAEA, Vienna, Austria

Disclaimer

The report in its present state is "work in progress". Its availability to data testers is intended for offering the opportunity to provide comments and feedback. In several cases the results are incomplete.

May 2018

Contents

1 Introduction

Extensive validation work on the CIELO [1] and ENDF/B-VIII.0 evaluations [2] identified a few problems with iron evaluations [3], the most damaging one being an underestimation by up to 30% of the transmitted fast neutron flux with energies from 0.85 up to around 10 MeV (e.g., see Fig.32 in Ref.[3]). This underestimation was first pointed out by S. Simakov [3] using neutron leakage measurements of ^{252}Cf(sf) source inside thick iron spherical shells carried out at IPPE, Russia. The underestimation of the neutron leakage was also observed for measurements with a D-T 14-MeV neutron source using the same spherical shells in the outgoing neutron range from 0.85 to 4 MeV (see Fig.35 in Ref.[3]).

Modifications of the ENDF/B-VIII.0/CIELO iron evaluations have been undertaken to address identified shortcomings within the INDEN project and will be described elsewhere. Total, elastic and inelastic neutron cross sections and angular distributions have been modified for ^{56}Fe nucleus from 0.85 up to 10 MeV of neutron incident energy. Additionally, neutron capture on ^{54}Fe and inelastic neutron scattering cross sections on ^{57}Fe were modified in the corresponding resonance regions. This report is devoted to a comprehensive comparison with a broad group of integral benchmarks that are openly available. The libraries included in the comparison are:

"e71" ENDF/B-VII.1 library serving as the basic reference.

"e80b6" ENDF/B-VIII.0 library

"jeff33" JEFF-3.3 library

"e80b6Fe_Xoj" INDEN improved iron evaluation replaced in ENDF/B-VIII.0 library.

The benchmark models are based on the information in the ICSBEP Handbook and the SINBAD package available from the OECD/NEA Data Bank, and information provided through private communications.

2 Leakage Spectra Experiments with ^{252}Cf Source

2.1 ALARM-CF-FE-SHIELD-001

Six iron spheres of different thicknesses with a ^{252}Cf source at the centre are described in the ICSBEP Handbook. ^{252}Cf(sf) neutron spectrum is a reference spectrum which is very well known. The neutron leakage spectra from the spheres were measured. The results for the whole energy range are shown in Figure 2.1.1 for all spheres. Expanded views of the resonance range, the 1 – 2 MeV and 2 – 5 MeV energy ranges are shown in Figures 2.1.2 to 2.1.4. respectively.

The figures indicate that with all libraries there are systematic deviations in the resonance range below 850 keV energy of leaked neutrons, which is understandable since the resonance parameters in all of them are rather similar. The worst cases are the region just below 100 keV in the thin spheres and the region near 300 keV in the thick spheres. There is a need to improve the resonance analysis of the iron isotopes.

---

[1] M.B. Chadwick et al., CIELO Collaboration Summary Results: International Evaluations of Neutron Reactions on Uranium, Plutonium, Iron, Oxygen and Hydrogen, *Nuclear Data Sheets* **148** (2018) 189-213.
[2] D.A. Brown et al., ENDF/B-VIII.0: The 8th Major Release of the Nuclear Reaction Data Library with CIELO-project Cross Sections, New Standards and Thermal Scattering Data, *Nuclear Data Sheets* **148** (2018) 1–142.
[3] M. Herman, A. Trkov, R. Capote et al., Evaluation of Neutron Reactions on Iron Isotopes for CIELO and ENDF/B-VIII.0, *Nuclear Data Sheets* **148** (2018) 214–253.

In the energy region 1 – 2 MeV the spectrum prediction with the “e80b6” library is systematically low. The “jeff33” and “e80b6Fe_Xoj” calculations agree with measured values better than “e71”, but have a slight tendency to under-predict the spectrum near 1.5 MeV. The under-prediction is more pronounced in thicker spheres and extends slightly outside the experimental uncertainty band.

In the energy region 2 – 5 MeV the “e80b6” is again systematically low. The prediction with the “e80b6Fe_Xoj” library is perfect, while the “jeff33” library prediction is slightly high near 3.5 MeV for the thick spheres.

The underprediction of the spectrum between 1 MeV and 10 MeV with the “e80b6” library was already noted by Simakov in the ENDF/B-VIII.0 library description as noted in the Introduction. This was mainly caused by the increased inelastic cross section following the high-resolution measurements at Geel by Negret (2013), available in the EXFOR data base at the time of evaluation. Newer published data by Negret (2014) and measurements at the nELBE facility do not support such an increase. This was the biggest change to the ^{56}Fe cross sections, in addition to a slight decrease of the total cross section near 3 MeV.

Overall, the performance of the “jeff33” and “e80b6Fe_Xoj” libraries on these benchmarks is quite good, and represents a large improvement over ENDF/B-VIII.0 for fast neutron leakage above 850 keV.

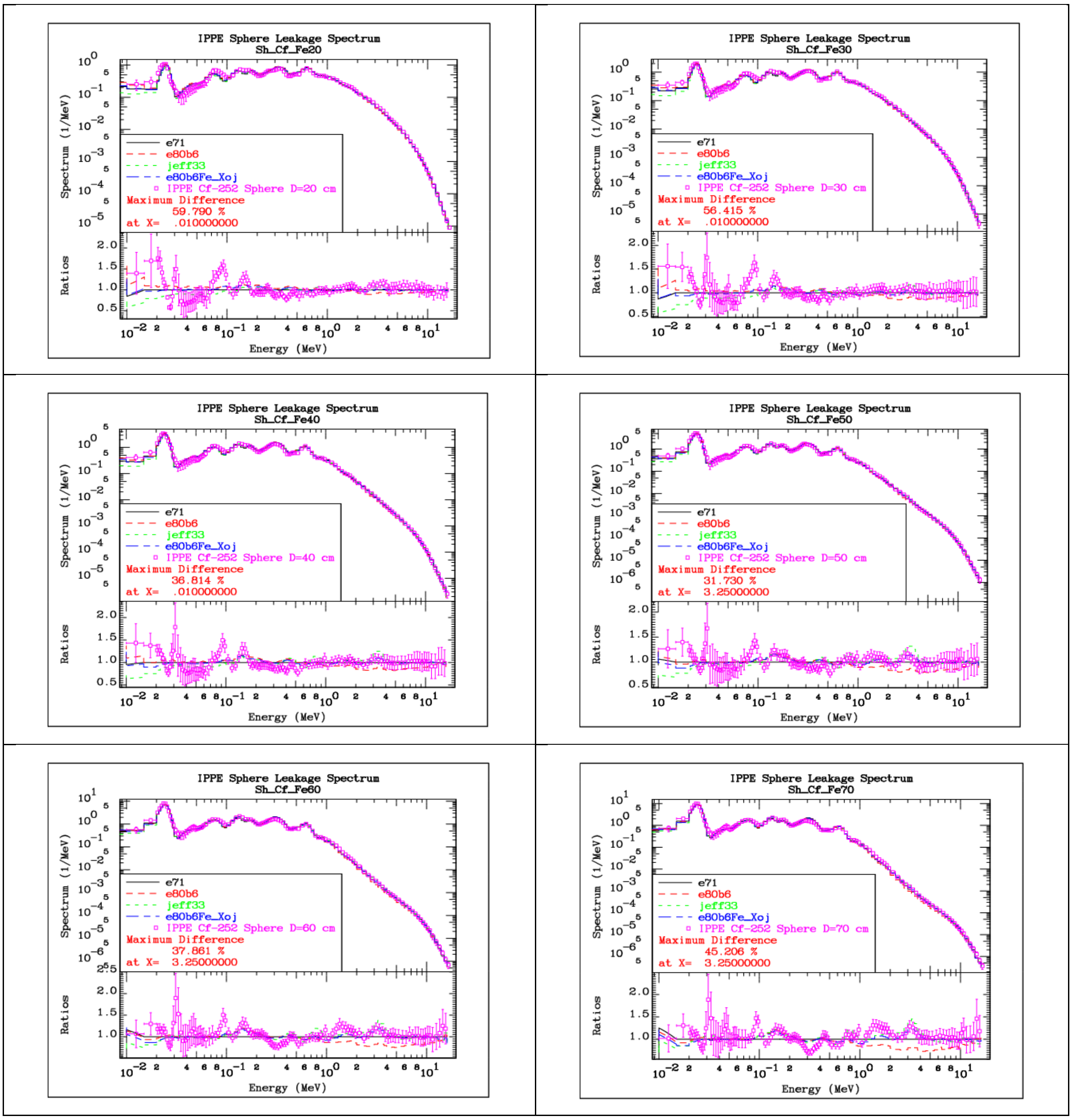

FIG. 2.1.1: Leakage spectra from the IPPE iron spheres with a ^{252}Cf source at the centre.

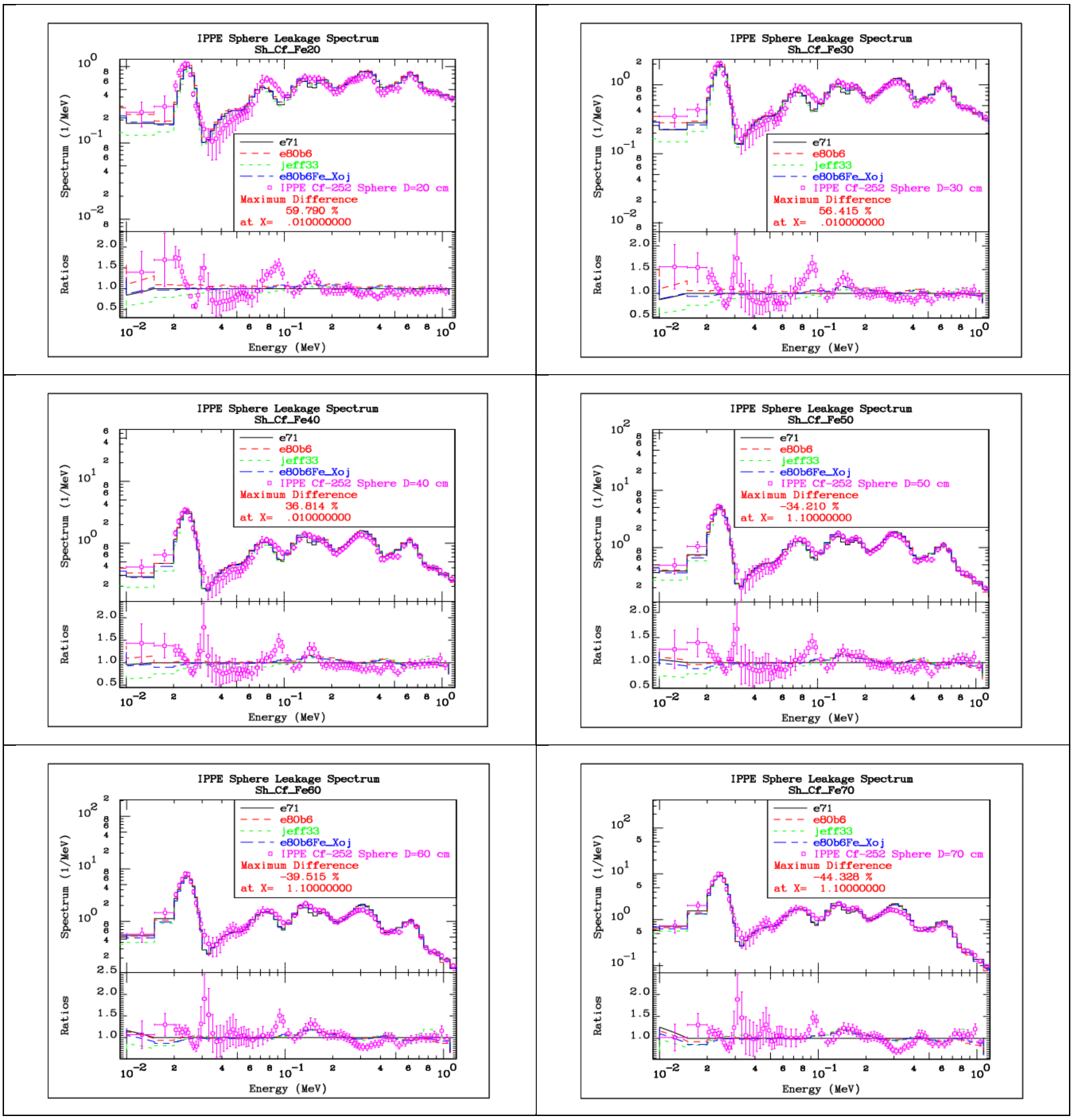

FIG. 2.1.2: Neutron leakage with energies from 0.01 up to 1 MeV from the IPPE iron spheres with a ^{252}Cf source at the centre.

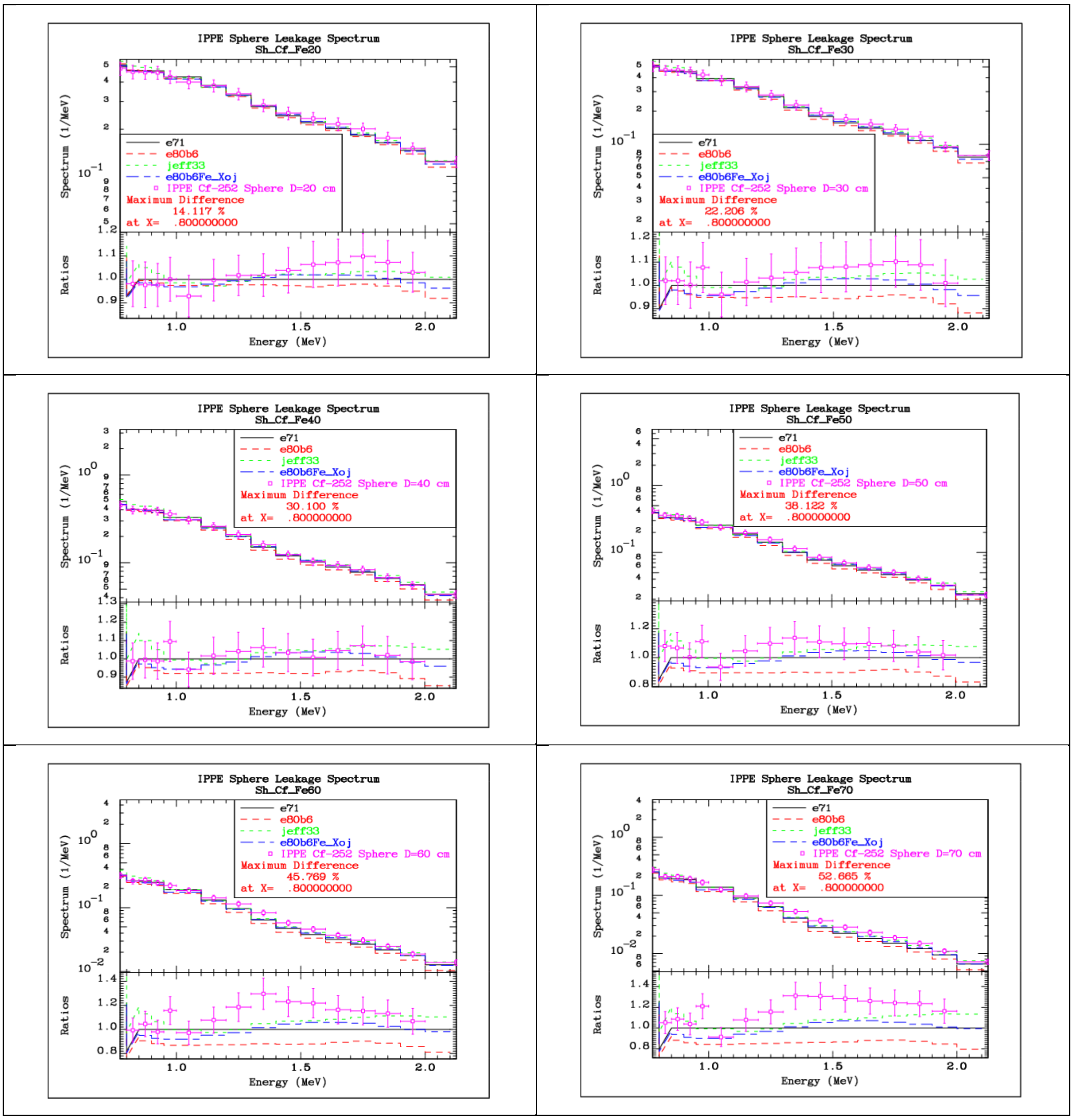

FIG. 2.1.3: Neutron leakage with energies from 0.85 up to 2.2 MeV from the IPPE iron spheres with a ^{252}Cf source at the centre.

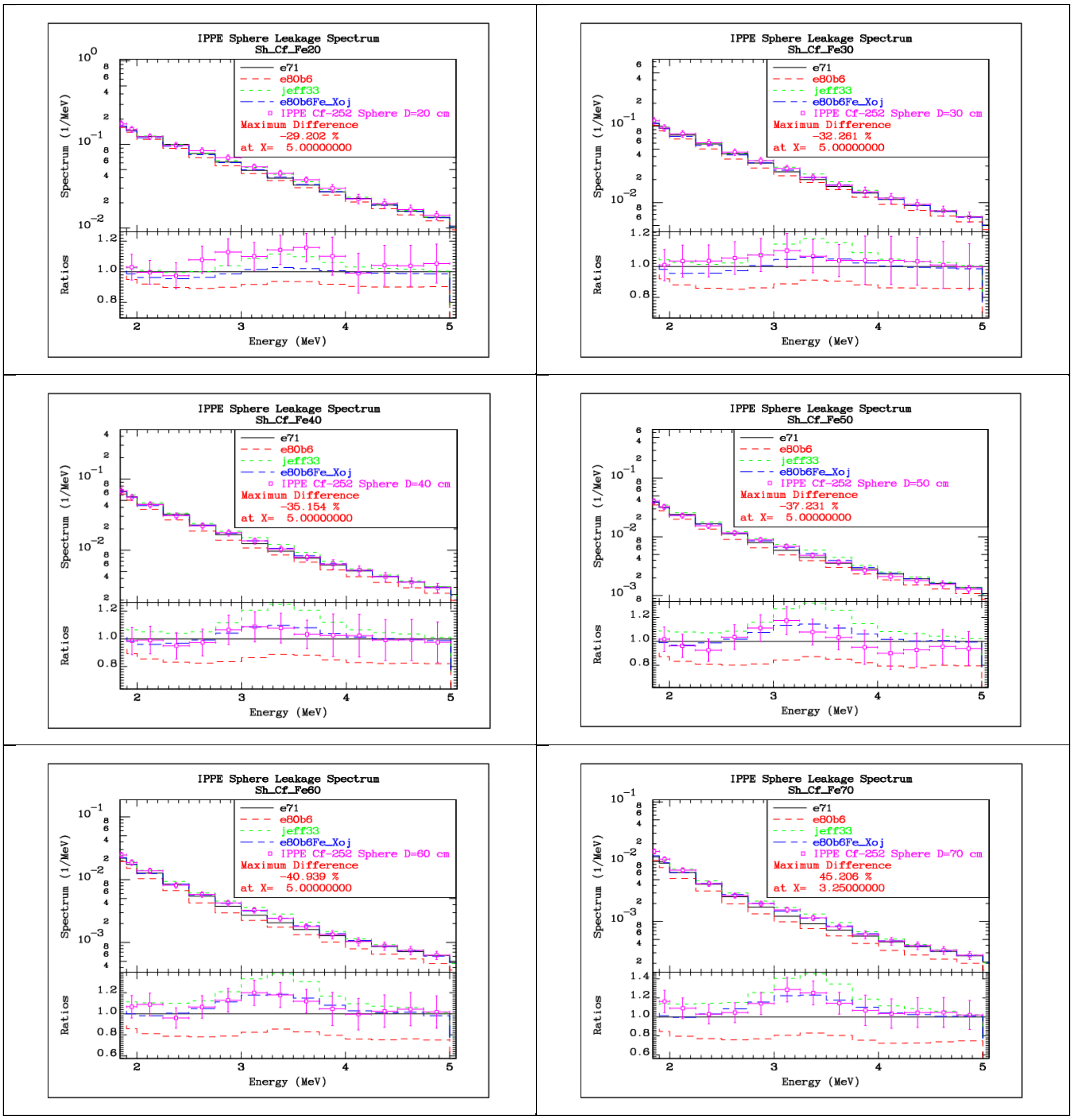

FIG. 2.1.4: Neutron leakage with energies from 1.8 up to 5.0 MeV from the IPPE iron spheres with a ^{252}Cf source at the centre.

2.2 Rez ^{252}Cf Leakage Spectra Experiments

Through private communication some information about the measurements on a one-meter diameter shells were obtained, but without the numerical data from the measurements and insufficient details to develop computational models. The benchmark would be of interest for an independent verification of the similar benchmarks performed at IPPE that are described in the previous section.

3 Leakage Spectra Experiments with D-T Source

3.1 Oktavian

The leakage spectra measurements on the Oktavian facility were done at the Osaka University in 1983. The benchmark specifications can be found in the SINBAD compilation. The special feature of the benchmark is that the low-energy part of the spectrum was measured. The calculated spectra are shown in Figure 3.1.1. The uncertainties in the measured spectrum in the MeV energy range are too large to be useful for data validation. (Note: in the current analysis no resolution-broadening was accounted for). Some suggestions for analysing these benchmarks were reported (e.g. The OKTAVIAN TOF experiments in SINBAD: Evaluation of the experimental uncertainties, Alberto Milocco, Andrej Trkov, Ivan A. Kodeli, Annals of Nuclear Energy 37 (2010) 443–449).

The benchmark confirms that the “e80b6” library predicts a significantly lower spectrum in the energy range 1 MeV to 4 MeV compared to other evaluations, as discussed in the previous section.

There is distinct overprediction of the neutron spectrum near 300 keV with all libraries, as already noted in the previous sections.

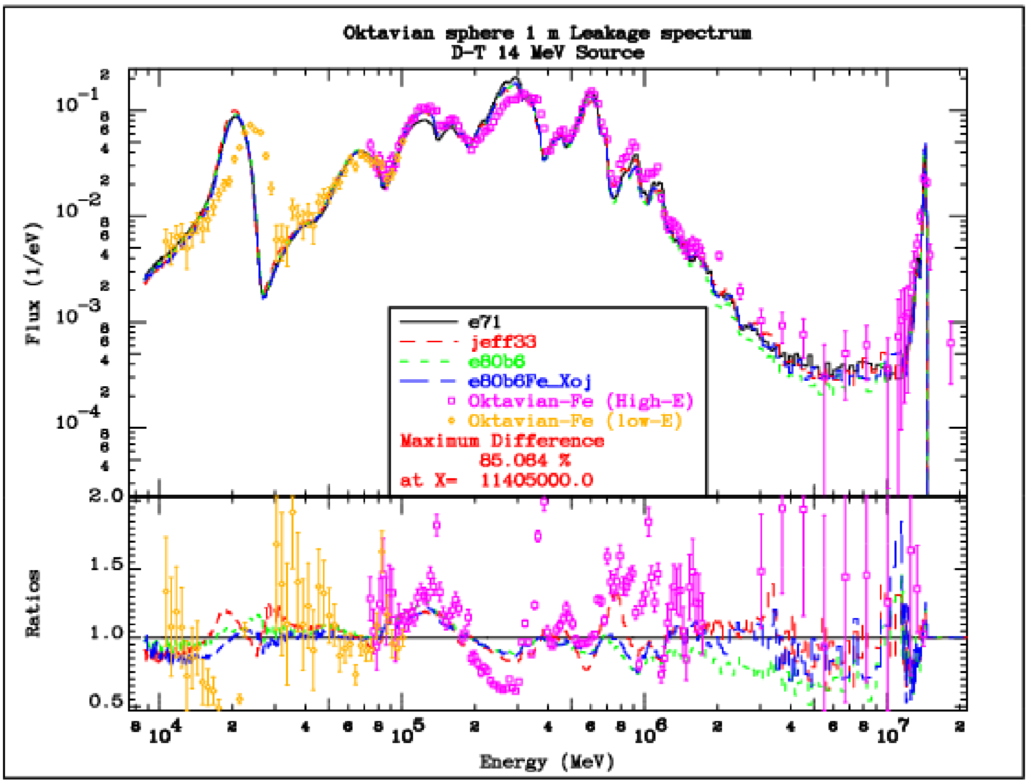

FIG. 3.1.1: Leakage spectrum from the Oktavian iron sphere with a D-T source at the centre.

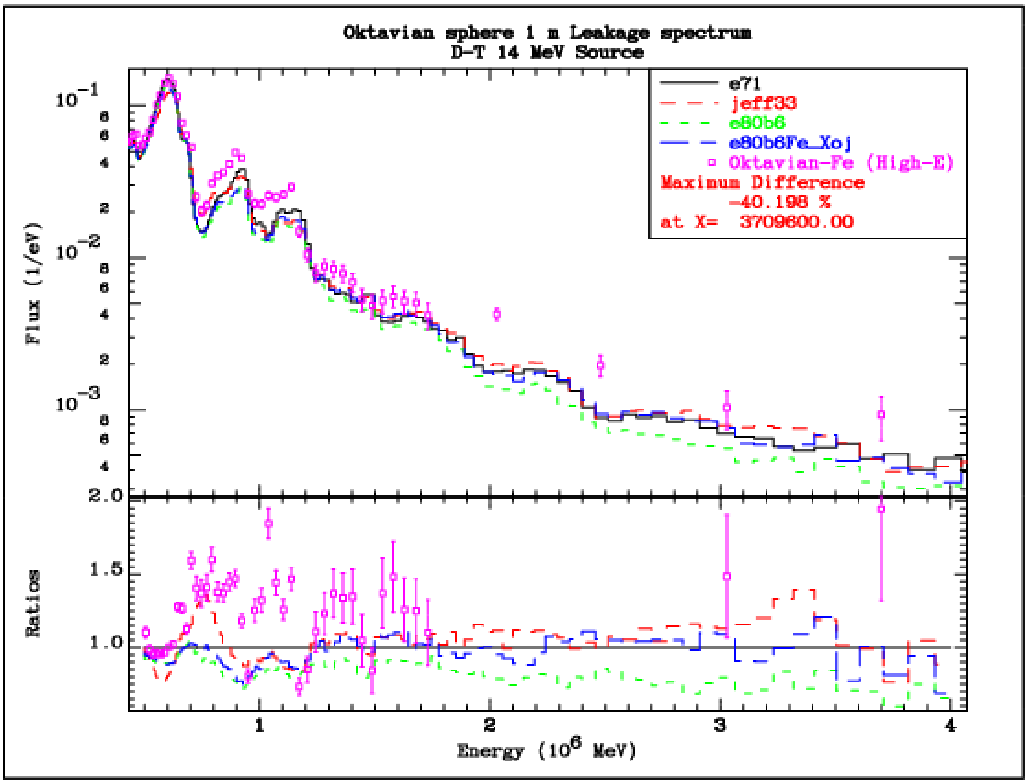

FIG. 3.1.2: Leakage spectrum in the MeV energy range from the Oktavian iron sphere with a D-T source at the centre.

3.2 Leakage spectra measurements at the Ohio State University

No information could be obtained other than the reference:

(Novel Investigation of Iron Cross Sections via Spherical Shell Transmission Measurements and Particle Transport Calculations for Material Embrittlement Studies, Michael T. Wenner, Alireza Haghighat, James M. Adams, Allan D. Carlson, Steven M. Grimes and Thomas N. Massey, NUCLEAR SCIENCE AND ENGINEERING: 170, 207–233, 2012)

3.3 LLNL pulsed sphere experiments (to be updated)

The LLNL pulsed sphere experiments were analysed by several authors and are documented in various reports. Numerical data from the measurements are available in (C. Wong, J. D. Anderson, P. Brown, L. F. Hansen, J. L. Kammerdiener, C. Logan and B. Pohl, LIVERMORE PULSED SPHERE PROGRAM: PROGRAM SUMMARY THROUGH JULY 1971, UCRL-51144, Rev. I, February 10, 1972). Data for the following cases are available:

llnl-fe09a	Small sphere with 4.46 cm outer radius (0.9 mean-free-path (m.f.p.) thickness, flight path 766 cm, NE213 detector at 30 degrees.
Llnl-fe09c	Small sphere with 4.46 cm outer radius (0.9 m.f.p. thickness, flight path 975.2 cm, NE213 detector at 120 degrees.
llnl-fe48a	Large sphere with 22.3 cm outer radius (4.8 mean-free-path (m.f.p.) thickness, flight path 766 cm, NE213 detector at 30 degrees.
Llnl-fe09c	Large sphere with 22.3 cm outer radius (4.8 m.f.p. thickness, flight path 975.2 cm, NE213 detector at 120 degrees.

The MCNP model is given as one of the examples supplied with the MCNP code. Computational models originally developed by S. Frankle were provided by D. Neudecker, together with numerical data from the measurements in computer-readable form, which are equal to the data in the original publication. The computational model for the “0.9 m.f.p” sphere with detector system “a” is practically identical to the one provided by O. Cabellos (private communication, April 2018). In the original publication there are data for a sphere of intermediate size (2.9 m.f.p.), but the data in computer-readable form and the models were not provided.

LLNL pulsed sphere results are usually presented in the time domain. For consistency, the same is shown in Figure 3.3.1. However, for data validation work such presentation is not intuitive because it is difficult to extract the information on the energy region where problems with the data might exist. The argument values of the spectrum can be converted to an effective energy scale by the time-of-flight methodology. Due to multiple scattering the conversion is not exact, but it does not affect the function value (i.e. the spectrum) at some particular effective-energy, as long as exactly the same method is used for converting the measured data and the data calculated in the time domain into the energy domain. The result is shown in Figure 3.3.2. By comparison with Figure 3.3.1 the C/E ratios are practically mirror images in the two sets of plots, but the plots in the energy domain are more informative regarding the energy regions in which problems are observed. It shows that at energies above 5 MeV the new evaluations reproduce better the measured spectrum, although the calculated spectrum is still over-predicted. This trend is reversed at lower energies.

In the expanded view in Figure 3.3.3, improved performance by all libraries and all measurements in the low-energy range is clearly demonstrated. In the thicker spheres the “e80b6Fe_Xoj” performs better than “e80b6”, but slightly worse than “jeff33” near the lowest measured energies.

Spectrum is the lowest near 11 MeV, as seen from Figure 3.3.4. In this energy range the performance is hard to judge. All libraries perform better than “e71”. The “jeff33” library seems to be marginally better. A similar conclusion follows for the highest measured energies, as shown in Figure 3.3.5.

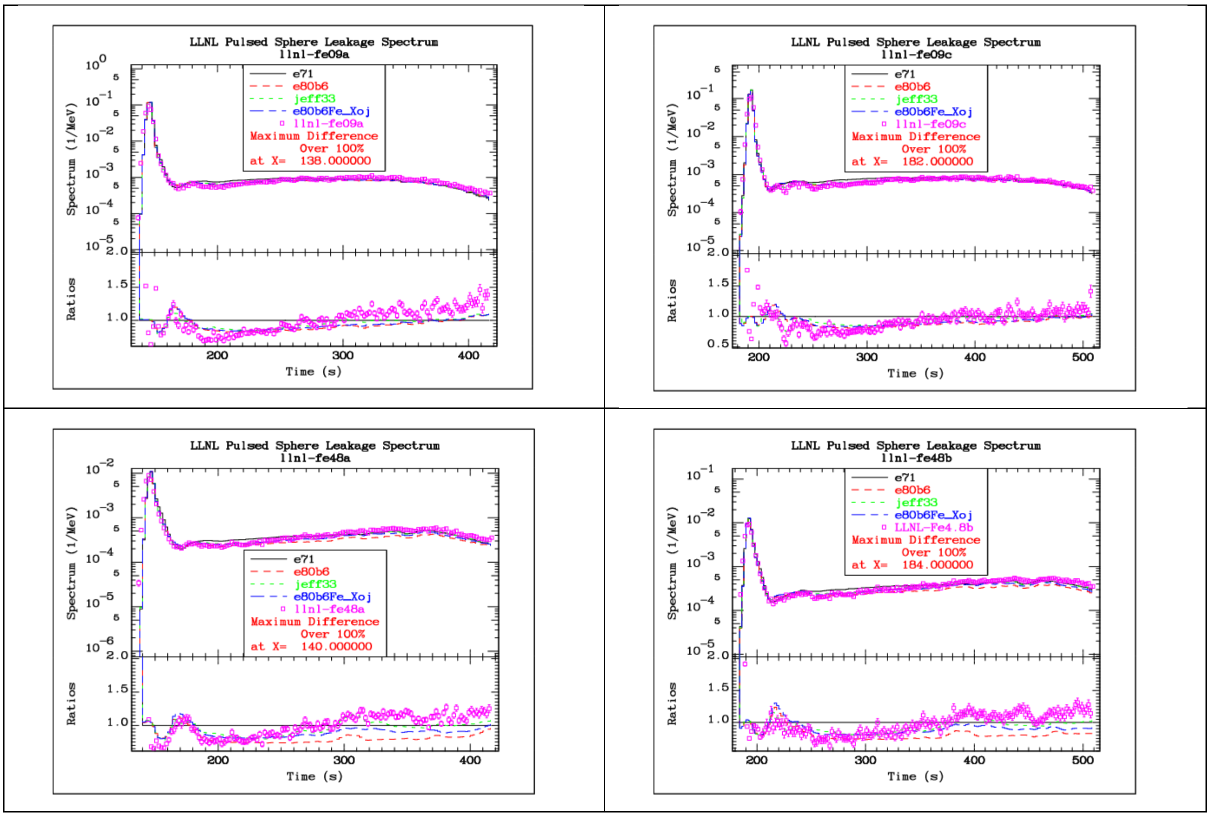

FIG. 3.3.1: LLNL pulsed-sphere iron benchmark experiments represented in the time domain.

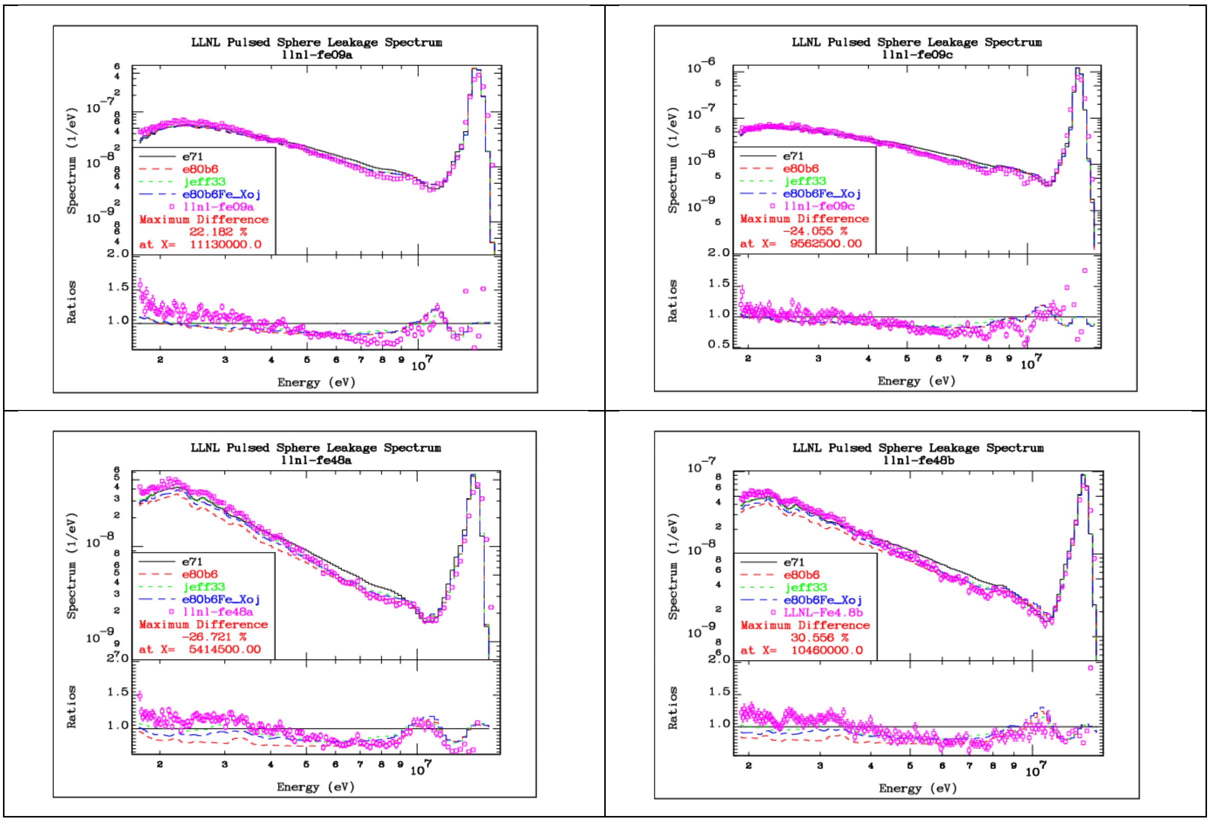

FIG. 3.3.2: LLNL pulsed-sphere iron benchmark experiments represented in the energy domain.

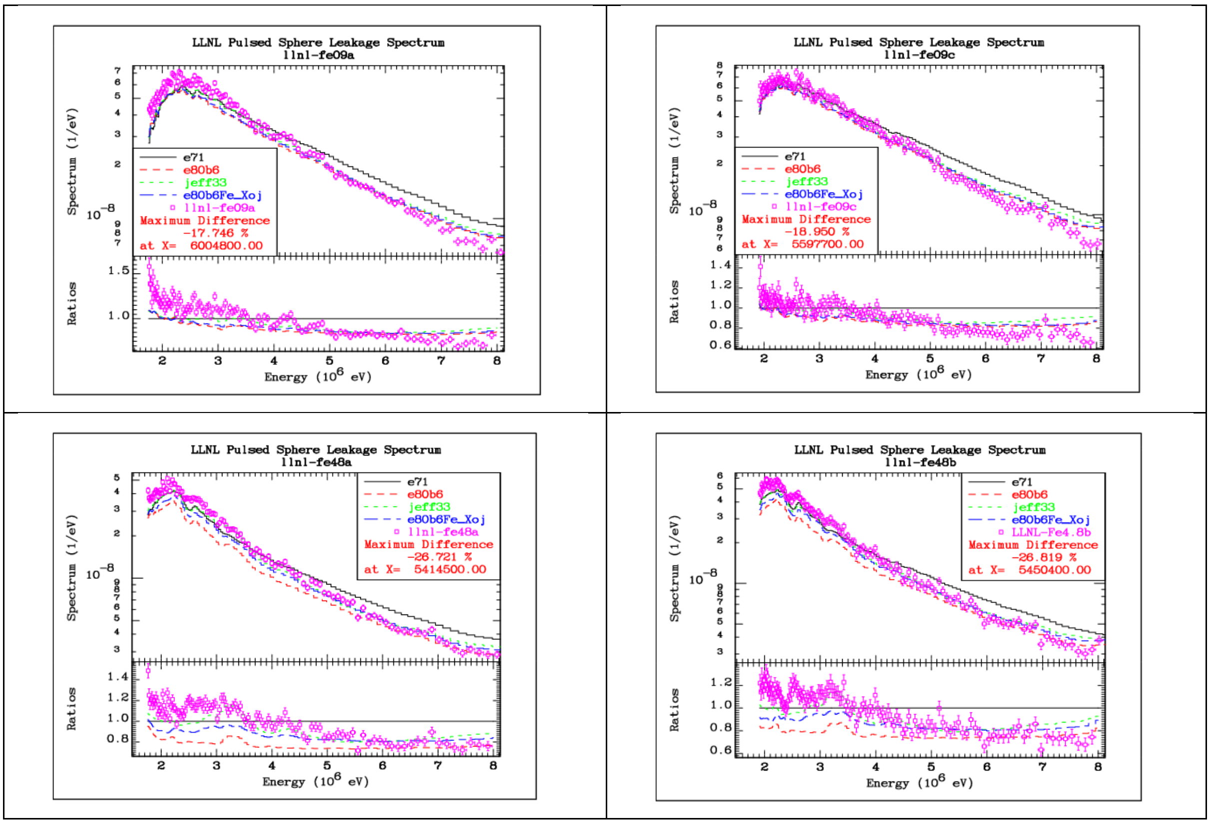

FIG. 3.3.3: LLNL pulsed-sphere iron benchmark experiments with expanded scale at low energies.

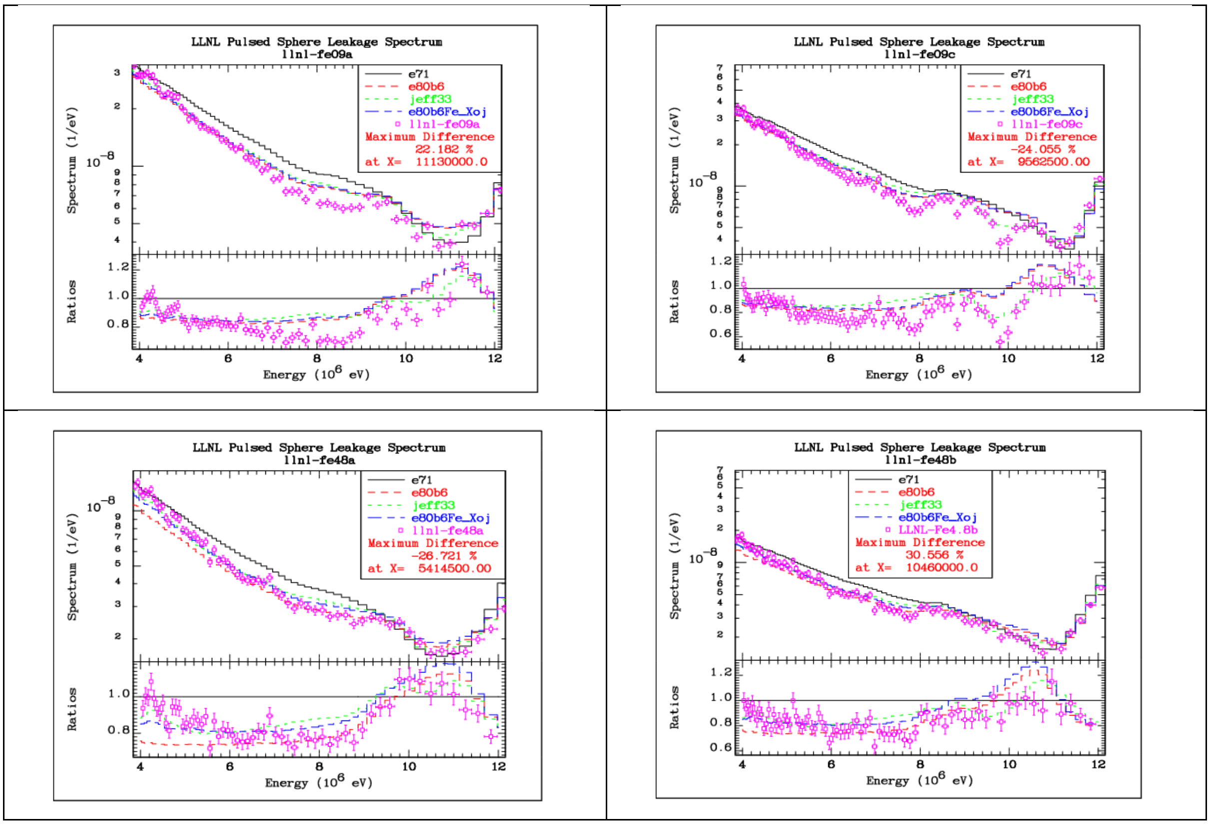

FIG. 3.3.3: LLNL pulsed-sphere iron benchmark experiments with expanded scale at intermediate energies.

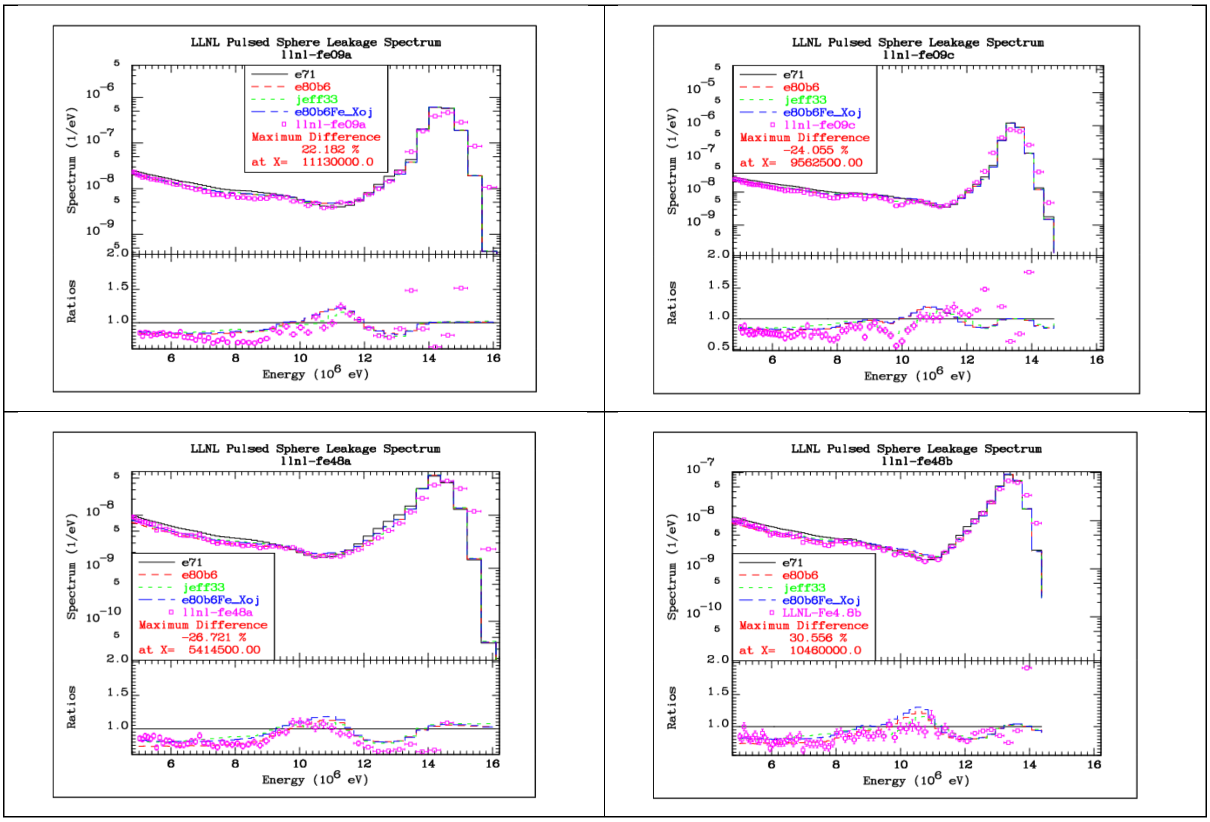

FIG. 3.3.3: LLNL pulsed-sphere iron benchmark experiments with expanded scale at high energies.

In drawing conclusions regarding the LLNL pulsed iron spheres benchmarks one has to consider also the similar set of experiments performed at IPPE, which are described in the next section. Specifically, the “0.9 m.f.p” sphere is similar to the first IPPE sphere analysed in Section 3.4 and the 4.9 m.f.p sphere is similar to the fourth IPPE sphere. The trend of under-predicting the spectrum in the low-energy tail of the measurement (starting at about 2 MeV) is not confirmed in the IPPE experiments.

3.4 Leakage spectra from IPPE spheres with a D-T source

The iron sphere experiments were carried out at the 14 MeV facility in IPPE, Obninsk, Russia. A pulsed beam of deuterons was injected into a solid Titanium - Tritium target and generated a 14 MeV neutron source at the centre of the iron spheres. Leakage spectra from five spheres were measured, as specified in Table 3.4.1.

The experiments are included in the SINBAD documentation. The models for MCNP and the analysis procedures are included (A. Milocco, A. Trkov, P6 – Iron Spheres Experiments, IJS-DP-9532, Jožef Stefan Institute, Slovenia, 2007). In the current work the results are based on the cell-flux tally in the time-domain with external resolution-broadening using a Gaussian resolution function of 2.1 ns width and subsequent conversion into energy domain using the specified effective flight path.

TABLE 3.4.1. IRON SPHERE CHARACTERISTICS FROM THE IPPE EXPERIMENT WITH A D-T SOURCE

Sphere	R_outer	R_inner	Diameter	Thickness	S/V
No.	[cm]	[cm]	[cm]	[cm]	[%]
1	4.5	2	9	2.5	10.6
2	12	4.5	24	7.5	3.3
3	12	2	24	10	3.7
4	20	1.9	40	18.1	0.9
5	30	2	60	28	0.8

The comparison between the calculations using different libraries and measurements over the entire energy range is shown in Figure 3.4.1.

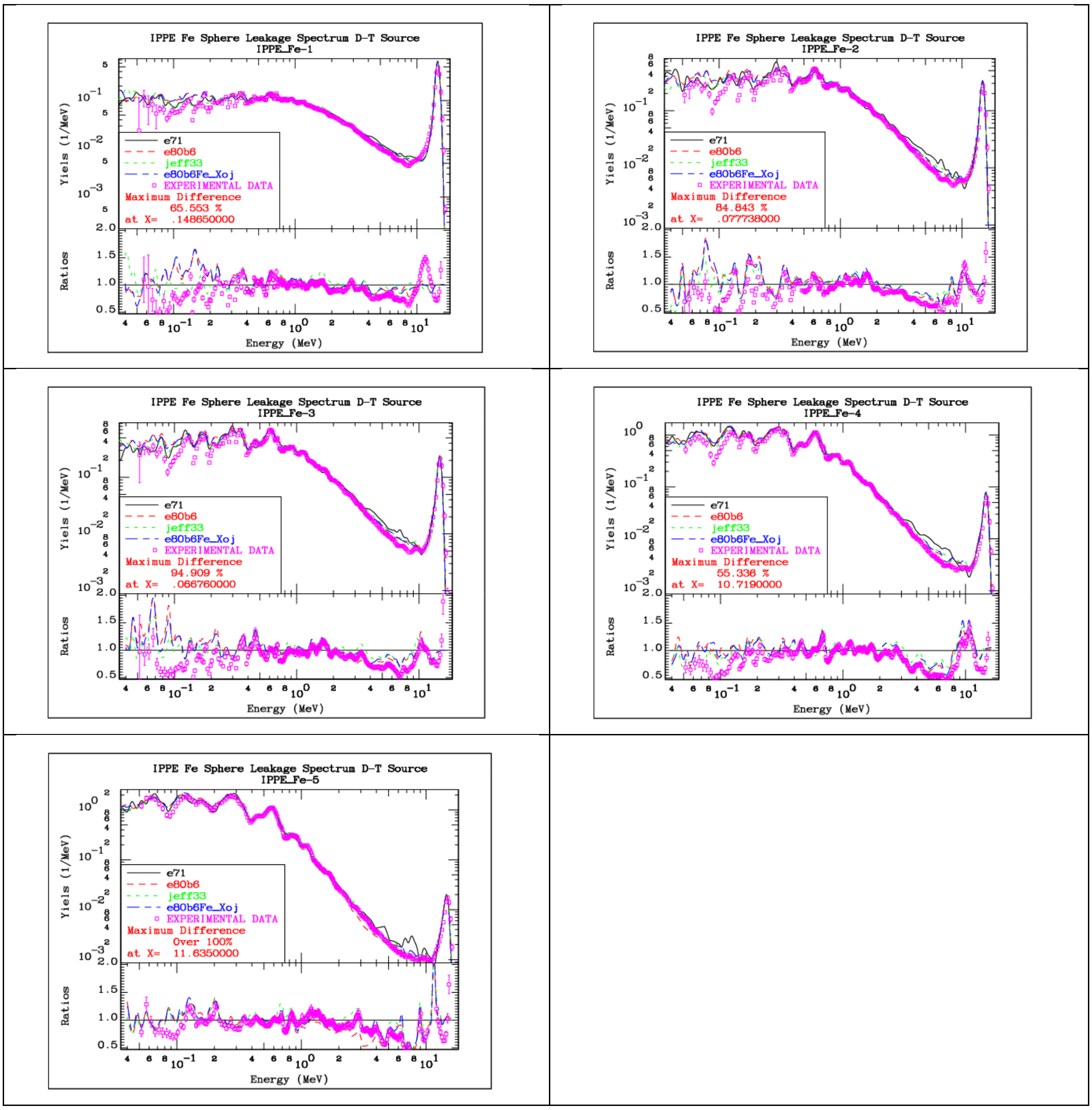

FIG. 3.4.1: Leakage spectra from the IPPE iron spheres with a D-T source at the centre.

Refinement of the displayed energy range in the resonance region is shown in Figure 3.4.2. The largest sphere is somewhat comparable to the Oktavian experiment. It confirms a slight over-prediction of the leakage spectrum near 300 keV, although it is not as pronounced as in the Oktavian experiment. At lower energies there is considerable scattering of the measured data, particularly for the thinner spheres.

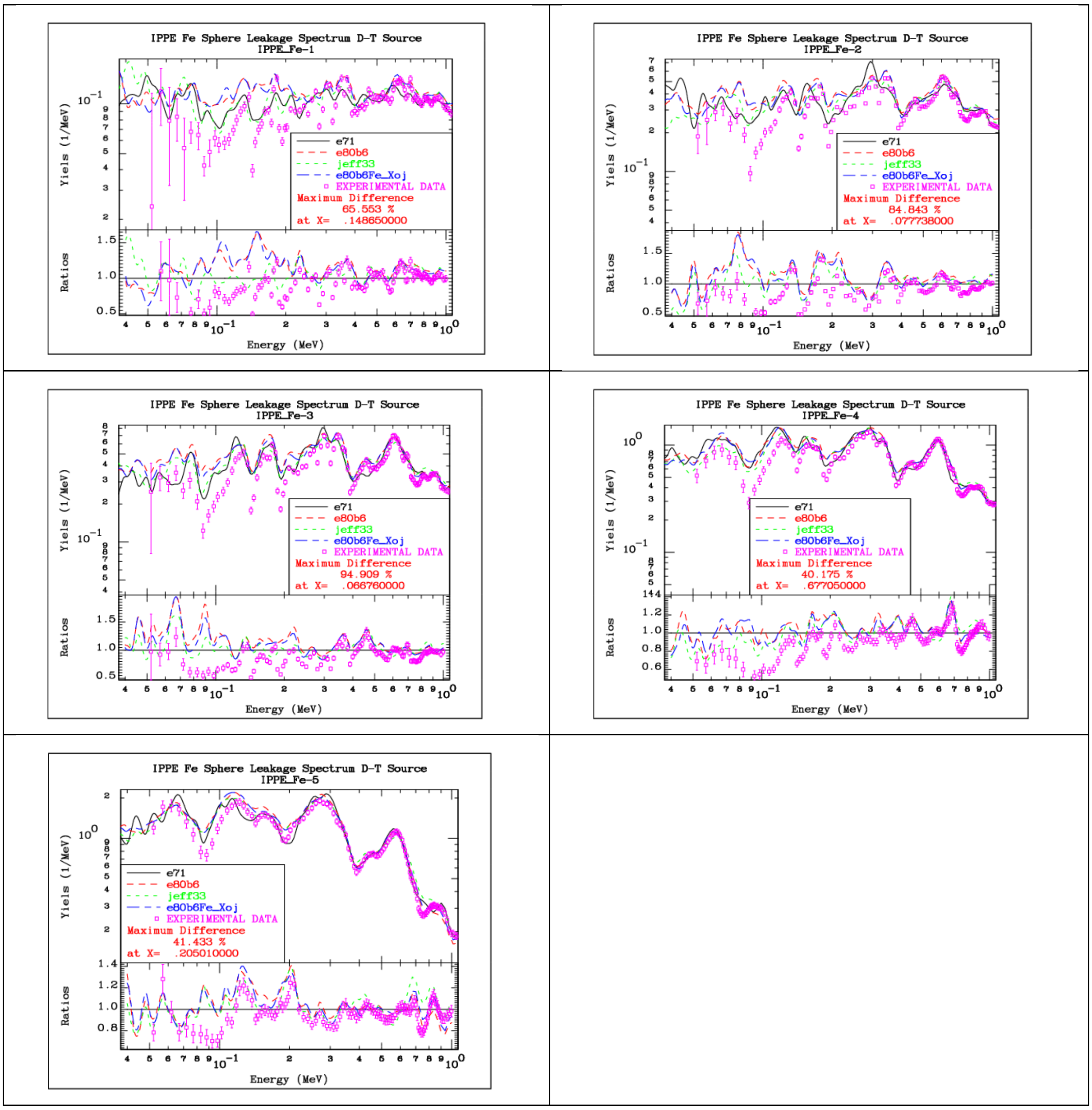

FIG. 3.4.2: Leakage spectra from the IPPE iron spheres with a D-T source at the centre.

Above the resonance range the “e80b6” and “e80b6Fe_Xoj” represent considerable improvement compared to “e71”, although one can observe some differences at different sphere thicknesses. The IPPE_Fe-3 case also shows that the improved “e80b6Fe_Xoj” is significantly better than “e80b6”.

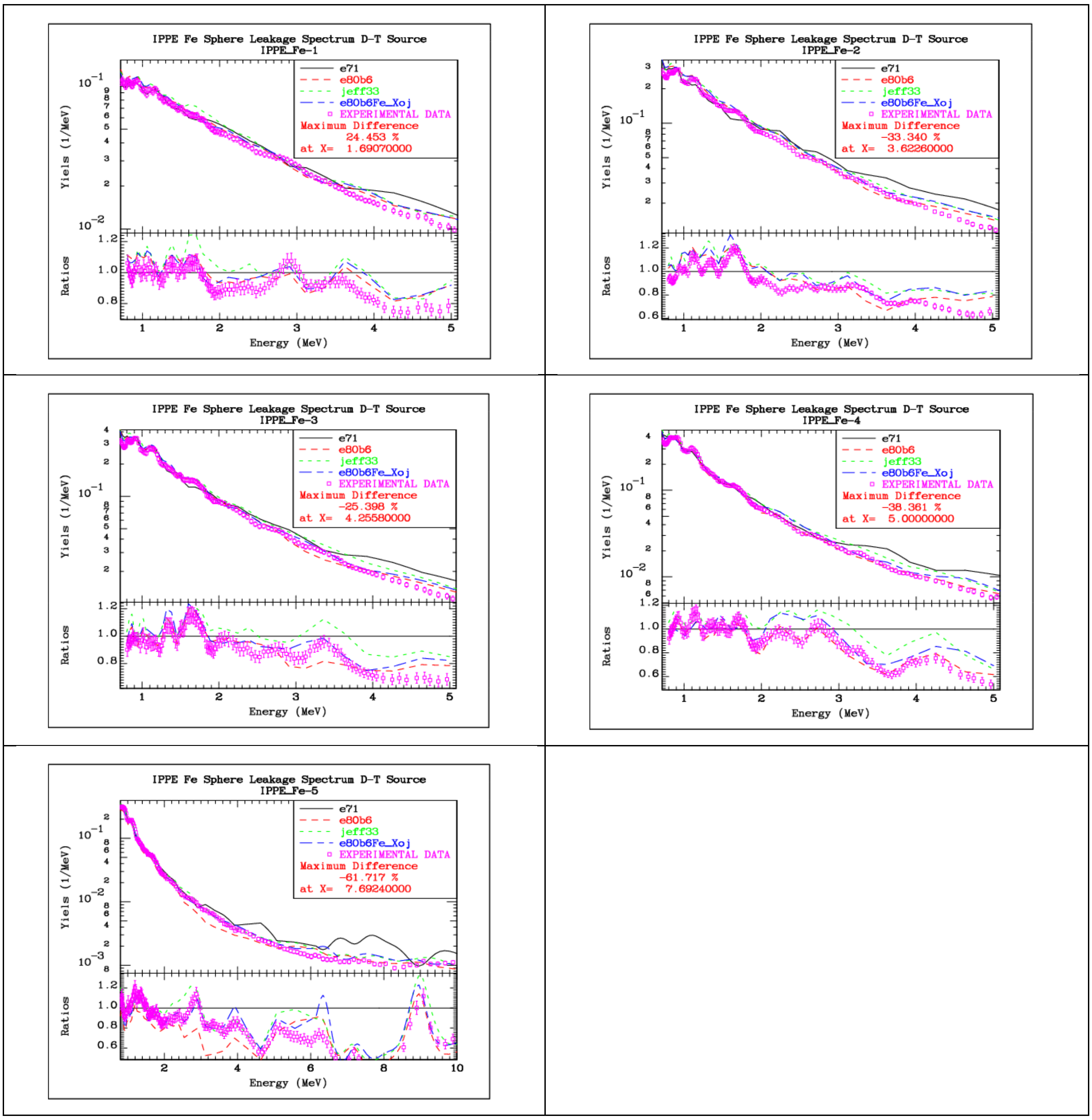

FIG. 3.4.3: Leakage spectra from the IPPE iron spheres with a D-T source at the centre.

Above 5 MeV the “e80b6” and “e80b6Fe_Xoj” represent considerable improvement compared to “e71”, especially for the thick iron spheres. Improved agreement is confirmed between measurements and calculations with the newer libraries below 9 MeV, similar to the one observed in the LLNL-Fe pulsed sphere experiment described in Section 3.3.

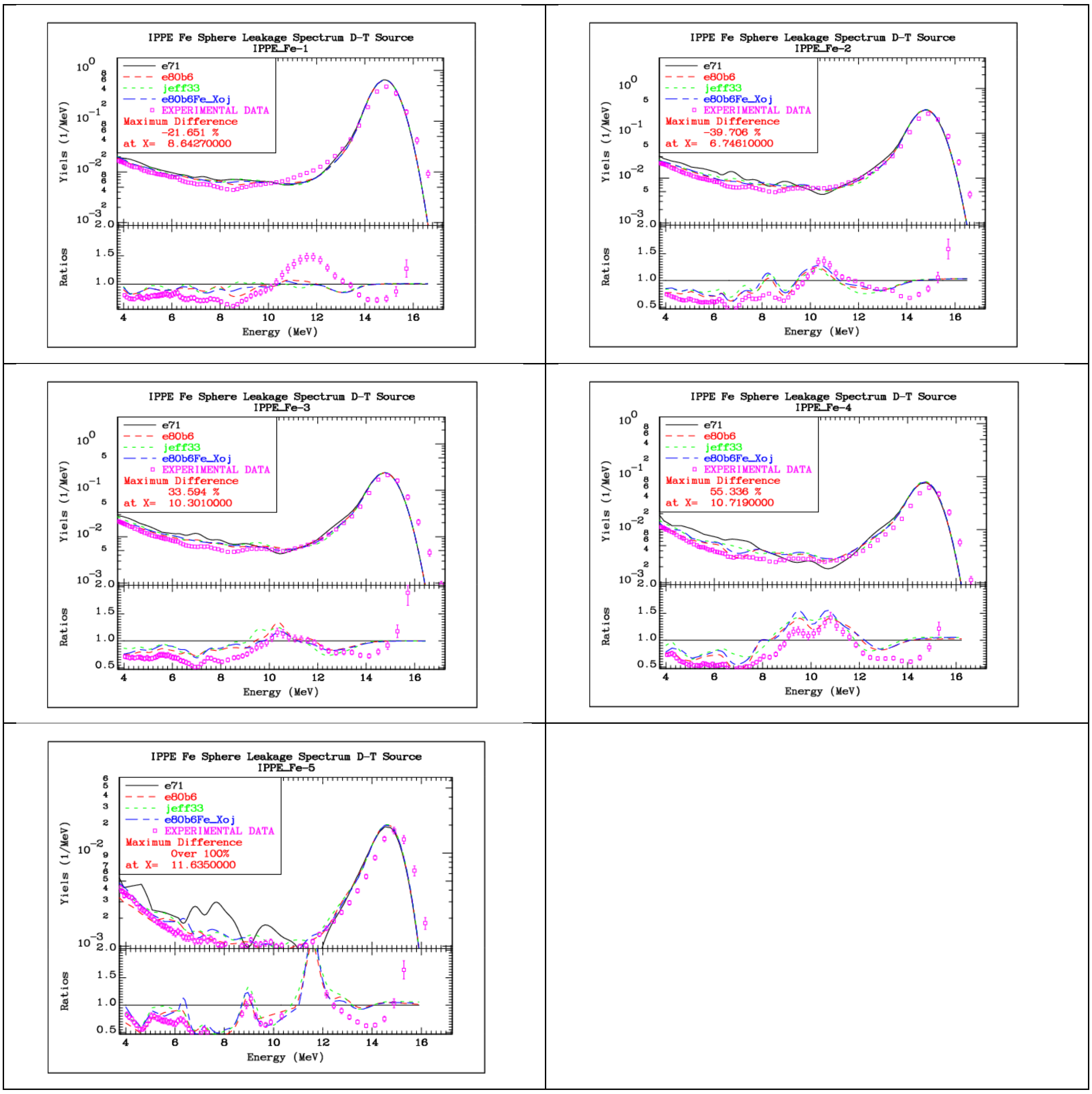

FIG. 3.4.4: Leakage spectra from the IPPE iron spheres with a D-T source at the centre.

4 Iron Broomstick experiments

4.1 FUND-IPPE-VDG-MULT-TRANS-001

The experiments at IPPE consisted of stacked iron samples of about 5 cm diameter and length ranging from 0.4 cm to 50 cm bombarded by a neutron beam from a tritiated lithium target bombarded with a proton beam (denoted p+Li(T) source for short). The energy of the proton beam was varied to obtain a quasi-monoenergetic beam of neutrons.

The experiments described in the ICSBEP Handbook give detailed results, specifying the applicable energy ranges for each measurement and the combined sample thicknesses. The computational model assumes that the spectrum is flat in the specified energy range, which is an approximation. In principle, any neutron interaction removes neutrons from the beam so that it does not reach the detector. One of the models suggested in the Handbook follows this approach in a model using the PrePro codes, but this is an approximation that ignores multiple scattering. In the present analysis a separate calculation was performed with MCNP for each of the 25 sample thicknesses using different data libraries.

In the trial analysis an attempt was made to display data comparison as a function of energy for each sample thickness. The results were obscured most likely by the approximation of a flat spectrum. In the second analysis we compared the attenuation factors as a function of sample thickness for broad energy intervals. A similar analysis was reported by Andrew Pavlou and Jason Thompson at the 2017 CSEWG Meeting. Our observations regarding the ENDF/B-VII.1 and ENDF/B-VIII libraries are similar. In addition, we include the JEFF-3.3 and the INDEN evaluations for the iron isotopes in our analysis. The results for different energy regions are shown in Figure 4.1.1.

The experiment is essentially a transmission measurement, which is primarily sensitive to the total cross section. Ideally, the attenuation would be exponential as a function of sample thickness (i.e. straight line on a log-lin scale). Deviation from the exponential behaviour occurs due to spectral changes resulting from self-shielding, elastic and inelastic multiple scattering. As seen from Figure 4.1.1, the e80b6Fe_Xoj library is in very good agreement with the measurements up to 800 keV, which is the resonance range. Above the resonance range up to 1.4 MeV the experimental points seem to be more scattered. The agreement in the prediction with the e80b6Fe_Xoj library is still better than any other. Above 1.4 MeV the attenuation of neutrons is overpredicted with all libraries. The energy bins in this range are very broad, but it was checked that the trends, when considering detailed bin structure, are essentially the same.

Ideally, the multiple scattering effect in this type of measurements should be small since any scattering event would divert neutrons from the path and they would not reach the detector. A more important unexplored feature of the benchmark simulation is the flat flux approximation. Namely, within the specified energy interval the distribution of source neutrons is assumed to be uniform, while in reality, the shape of the spectrum of neutrons may change in p+Li(T) reaction as a function of incident proton energy. To check this quantitatively one would need to do trial runs for each sample thickness and each energy group with a realistic shape of the source spectrum from the p+Li(T) reactions. This analysis will be done in the future.

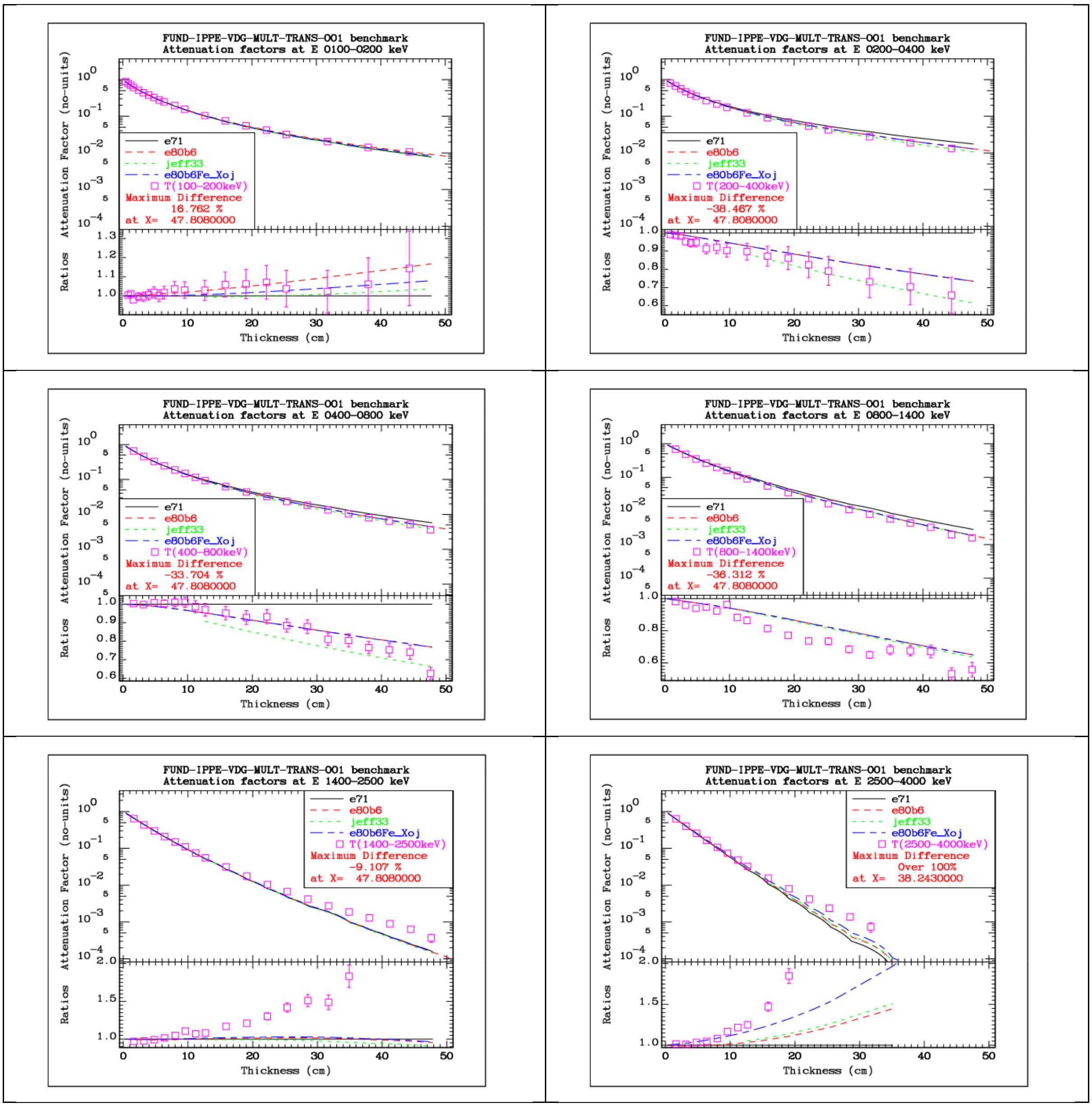

FIG. 4.1.1 Comparison of the dependence of the neutron flux attenuation coefficient as a function of sample thickness in different energy regions.

5 High-energy benchmarks

Several benchmarks are available in SINBAD, which still need to be included in the present analysis.

6 Criticality Benchmark Experiments from ICSBEP

Criticality benchmarks from the ICSBEP Handbook were selected based on the sensitivities to iron, as obtained from the DICE system developed at the OECD/NEA Data bank. A few additional ones that are often quoted by other authors were added. The list is given in Table 6.1.

The results are shown in Figure 6.1. Generally, the calculated multiplication factors k_{eff} lie practically within the quoted uncertainties, but there are a few exceptions, which are discussed below.

TABLE 6.1. LIST OF CRITICALITY BENCHMARKS FROM THE ICSBEP HANDBOOK

No.	ICSBEP Label	Short name	Common name
1	HEU-MET-FAST-013	hmf013	VNIITF-CTF-SS-13
2	HEU-MET-FAST-021	hmf021	VNIITF-CTF-SS-21
3	HEU-MET-FAST-024	hmf024	VNIITF-CTF-SS-24
4	HEU-MET-FAST-087	hmf087	VNIITF-CTF-Fe
5	HEU-MET-FAST-088	hmf088-001	FKBN-2/SS-PE-1
6	HEU-MET-FAST-088	hmf088-002	FKBN-2/SS-PE-2
7	HEU-MET-INTER-001	hmi001	ZPR-9/34
8	HEU-MET-THERM-013	hmt013-002	Planet_Fe-2
9	HEU-MET-THERM-015	hmt015	
10	IEU-MET-FAST-005	imf005	VNIIEF-CTF-5
11	IEU-MET-FAST-006	imf006	VNIIEF-CTF-6
12	LEU-COMP-THERM-042	lct042-001	lct042-001
13	LEU-COMP-THERM-042	lct042-002	lct042-002
14	LEU-COMP-THERM-043	lct043-002	IPEN/MB-01
15	LEU-MET-THERM-015	lmt015-001	RB-Vinca(01)
16	MIX-COMP-FAST-001	mcf001	ZPR-6/7
17	MIX-COMP-FAST-005	mcf005-s	ZPR-9/31
18	MIX-COMP-FAST-006	mcf006-s	ZPPR-2
19	PU-MET-FAST-015	pmf015	BR-1-3
20	PU-MET-FAST-025	pmf025	pmf025
21	PU-MET-FAST-026	pmf026	pmf026
22	PU-MET-FAST-028	pmf028	pmf028
23	PU-MET-FAST-032	pmf032	pmf032
24	PU-MET-INTER-002	pmi002	ZPR-6/10
25	PU-MET-INTER-003	pmi003-001s	ZPR-3/58(U)
26	PU-MET-INTER-004	pmi004-001s	ZPR-4/59(Pb)
27	IEU-COMP-INTER-005	ici005	ZPR-6/6A

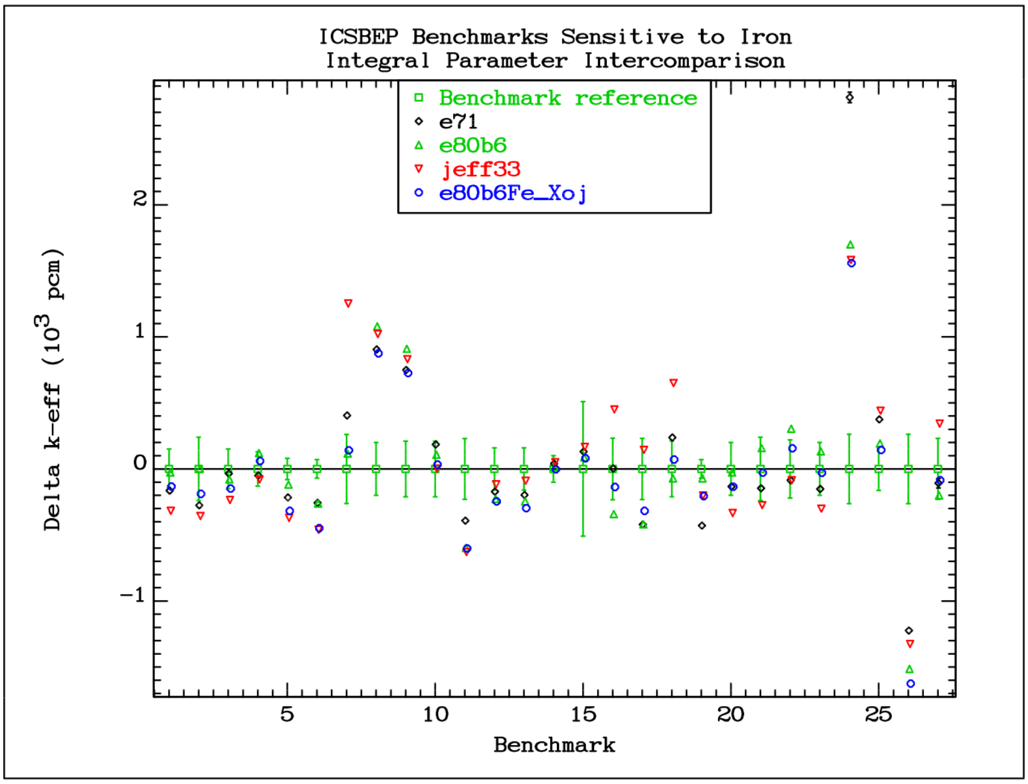

FIG. 6.1: Comparison of the differences between the calculated and the benchmark k_{eff} using different evaluated nuclear data libraries.

6.1 HEU-MET-FAST-088

The benchmark consists of two cases (number 4 and 5 in Figure 6.1), performed at the criticality test facility FKBN-2 at VNIITF in 1988; both cases are predicted low in reactivity. The sensitivity coefficients of the secondary material components of Case-1 is given in Table 6.1.1, which show that the only reactions of any significance are the elastic and the capture cross sections of ^{54}Fe. The elastic cross section is constrained by the total and does not allow for large changes. The capture cross section is not so well defined, but the sensitivity coefficient shows that a uniform reduction of the capture cross section by 50% would only increase the reactivity by about 100 pcm, which is still far from the observed reactivity. We were not able to identify the root cause of the problems which may lie in the benchmark specifications, the model or the nuclear data. Further studies are warranted.

TABLE 6.1.1. SENSITIVITIES TO THE CROSS SECTIONS OF THE MINOR CONSTITUENTS OF THE HEU-MET-FAST-088-001 BENCHMARK.

			Thermal	Epithermal	Fast	Total
HEU-MET-FAST-088-001	Fe54	capture	-0.0011	-0.0001	-0.0009	-0.0021
HEU-MET-FAST-088-001	Fe54	elastic-P1	0	0	-0.0008	-0.0008
HEU-MET-FAST-088-001	Mn55	capture	-0.0006	-0.0001	0	-0.0007
HEU-MET-FAST-088-001	Fe57	capture	-0.0004	-0.0001	0	-0.0005
HEU-MET-FAST-088-001	Fe57	elastic-P1	0	0	-0.0002	-0.0002
HEU-MET-FAST-088-001	Mn55	elastic-P1	0	0	-0.0002	-0.0002
HEU-MET-FAST-088-001	Si28	elastic-P1	0	0	-0.0001	-0.0001
HEU-MET-FAST-088-001	Cr52	elastic	0	0	0.0001	0.0001
HEU-MET-FAST-088-001	Fe58	inelastic	0	0	0.0001	0.0001
HEU-MET-FAST-088-001	Mn55	inelastic	0	0	0.0001	0.0001
HEU-MET-FAST-088-001	Mn55	elastic	0	-0.0002	0.0003	0.0001
HEU-MET-FAST-088-001	Fe58	elastic	0	0	0.0002	0.0002
HEU-MET-FAST-088-001	Si28	elastic	0	0	0.0004	0.0004
HEU-MET-FAST-088-001	Fe54	inelastic	0	0	0.0006	0.0006
HEU-MET-FAST-088-001	Fe57	inelastic	0	0	0.0009	0.0009
HEU-MET-FAST-088-001	Fe57	elastic	0	0	0.0011	0.0011
HEU-MET-FAST-088-001	Fe54	elastic	-0.0001	-0.0004	0.0046	0.0041

6.2 HEU-MET-INTER-001

This is the ZPR-9/34 benchmark from ANL (number 7 in Figure 6.1), which is one of the notorious outliers in many benchmarking exercises. It is sensitive to the minor constituent contributions in the energy window in the range 10 – 20 keV. The current iron evaluation with increased capture cross section in this energy window, where the cross section is very difficult to measure, provides a good balance that gives good reactivity prediction for this benchmark, but does not mean that all problems with the nuclear data are solved.

6.3 HEU-MET-THERM-015

The specifications for this pair of benchmark cases (number 8 and 9 in Figure 6.1) contain only pure iron, in addition to the fissile materials and moderators. Sensitivity coefficients were extracted from the DICE system of the OECD/NEA. Sensitivities in Table 6.3.1 show that only the sensitivity to the thermal capture cross section of ^{56}Fe is of any significance. The inelastic cross section in the post-ENDF/B-VIII evaluation of ^{56}Fe was reduced significantly, which is reflected in the reduction of the reactivity, but the reduction is by far insufficient compared to the discrepancy in the measured value.

TABLE 6.3.1. SENSITIVITIES TO THE IRON CROSS SECTIONS

Benchmark	Nuclide	Reaction	Thermal	Epithermal	Fast	Total
HEU-MET-THERM-015-001	Fe56	capture	-0.0288	-0.0016	-0.0001	-0.0305
HEU-MET-THERM-015-001	Fe57	capture	-0.0006	0	0	-0.0007
HEU-MET-THERM-015-001	Fe54	capture	-0.0016	-0.0001	-0.0001	-0.0018
HEU-MET-THERM-015-001	Fe54	elastic	0	0.0001	0.0001	0.0001
HEU-MET-THERM-015-001	Fe56	elastic	-0.0005	0.0016	0.0012	0.0023
HEU-MET-THERM-015-001	Fe57	inelastic	0	0	0.0001	0.0001
HEU-MET-THERM-015-001	Fe54	inelastic	0	0	0.0001	0.0001
HEU-MET-THERM-015-001	Fe56	inelastic	0	0	0.0022	0.0022

As shown in Table 6.3.2, the thermal cross section value of ^{56}Fe is already on the high side of the recommended value by Mughabghab, as well as by Firestone (Database of Prompt Gamma Rays from Slow Neutron Capture for Elemental Analysis, IAEA STI/PUB/1263, 2007). Further increase of the thermal capture cross sections is thus not warranted. This leads to the conclusion that the problem might be in the benchmark specifications or the models.

TABLE 6.3.2. THERMAL CAPTURE CROSS SECTIONS

	ENDF/B-VIII	Mughabghab	Firestone
Fe-54	2.25	2.25(18)	2.44(6)
Fe-56	2.61	2.59(14)	2.49(5)
Fe-57	2.48	2.5(3)	1.9(5)
Fe-58		1.30(3)	1.30(5)

6.4 PU-MET-FAST-015

The benchmark (number 19 in Figure 6.1) is an iron-reflected array of plutonium fuel rods. By itself it is not really a bad outlier, since its reactivity is underestimated by only about 200 pcm, but the assigned uncertainty is unreasonably small.

6.5 PU-MET-INTER-002

This is the ZPR-6/10 assembly from ANL (number 24 in Figure 6.1) with an intermediate spectrum, which is one of the notorious outliers in many benchmarking exercises. The changes to the capture cross sections of ^{56}Fe in the energy window in the range 10 – 20 keV significantly reduce the discrepancy in the predicted reactivity compared to the benchmark value, but the prediction is still high by about 1500 pcm.

6.6 PU-MET-INTER-004

The ZPR-3/59 assembly from ANL (number 26 in Figure 6.1) has a lead reflector. Several groups of benchmarks involving lead show large discrepancies, hence the root cause should be sought together with solving the problems with other lead-bearing assemblies.

Nuclear Data Section	E-mail: nds.contact-point@iaea.org
International Atomic Energy Agency	Fax: (43-1) 26007
Vienna International Centre, P.O. Box 100	Telephone: (43-1) 2600 21725
A-1400 Vienna, Austria	Web: http://nds.iaea.org